Superconductivity and bandwidth-controlled Mott metal-insulator transition in $1T$-$TaS_{2-x}Se_x$

R. Ang,[1,*] Y. Miyata,[2] E. Ieki,[2] K. Nakayama,[2] T. Sato,[2] Y. Liu,[3] W. J. Lu,[3] Y. P. Sun,[3,4] and T. Takahashi[1,2]

[1]*WPI Research Center, Advanced Institute for Materials Research, Tohoku University, Sendai 980-8577, Japan*

[2]*Department of Physics, Tohoku University, Sendai 980-8578, Japan*

[3]*Key Laboratory of Materials Physics, Institute of Solid State Physics, Chinese Academy of Sciences, Hefei 230031, China*

[4]*High Magnetic Field Laboratory, Chinese Academy of Sciences, Hefei 230031, China*

(Received 1 August 2013; revised manuscript received 19 September 2013; published 30 September 2013)

We have performed high-resolution angle-resolved photoemission spectroscopy (ARPES) of layered chalcogenide $1T$-$TaS_{2-x}Se_x$ to elucidate the electronic states especially relevant to the occurrence of superconductivity. We found a direct evidence for a Ta-5d-derived electron pocket associated with the superconductivity, which is fragile against a Mott-gap opening observed in the insulating ground state for S-rich samples. In particular, a strong electron-electron interaction-induced Mott gap driven by a Ta 5d orbital also exists in the metallic ground state for Se-rich samples, while finite ARPES intensity near the Fermi level likely originating from a Se 4p orbital survives, indicative of the orbital-selective nature of the Mott transition. Present results suggest that effective electron correlation and p-d hybridization play a crucial role to tune the superconductivity and Mott metal-insulator transition.

DOI: 10.1103/PhysRevB.88.115145 PACS number(s): 71.45.Lr, 71.20.−b, 71.30.+h, 79.60.−i

I. INTRODUCTION

In a low-dimensional electron system, the interplay between electron correlation, superconductivity, and charge order or charge density wave (CDW) is one of the central issues. The classical CDW order is well understood in terms of Fermi-surface nesting, owing to electron-phonon coupling in the framework of the Peierls mechanism. However, there often exists simultaneously strong electron-electron interaction in some materials, giving rise to the coexistence, competition, or collaboration of multiple orderings near the CDW order, and as a consequence evoking the phase diagram extremely complex in low-dimensional organic conductor[1,2] and high-temperature superconducting (SC) cuprates.[3,4]

Layered transition-metal dichalcogenide (TMD) $1T$-TaS_2 with CdI_2-type crystal structure [see Fig. 1(a)] provides an excellent platform, which displays an abundant diversity of ordered ground states, for exploring how various orderings cooperate or compete with CDW.[5–10] Particularly, pristine $1T$-TaS_2 undergoes a Mott insulator transition as it gets into a frozen CDW phase with $\sqrt{13} \times \sqrt{13}$ superstructure [see Fig. 1(b)]. Strikingly, the superconductivity is discovered in $1T$-TaS_2 in various conditions, e.g., under high pressure,[11] by introducing disorders in the crystal,[12] and by light Fe substitution in $1T$-$Fe_xTa_{1-x}S_2$ ($0 \leqslant x \leqslant 0.05$).[13,14] Very recently, the superconductivity is also discovered in $1T$-$TaS_{2-x}Se_x$ around $0.8 < x \leqslant 1.6$.[15] As derived from the previous transport properties [see Fig. 1(c)], the superconductivity of $1T$-$TaS_{2-x}Se_x$ in a wide x range surrounds within a nearly commensurate CDW (NCCDW) phase, while it is prominently isolated between a commensurate CDW (CCDW) Mott insulating phase and a CCDW metallic phase.[15] Spontaneously, one might ask why the superconductivity appears in $1T$-$TaS_{2-x}Se_x$. Indeed, $1T$-$TaS_{2-x}Se_x$ is an inherent solid-solution system and thus keeps a typical feature without essential consideration of carrier-density variation, which is likely to be irrelevant to the emergence of superconductivity. The intriguing question is what is the origin of the superconductivity in $1T$-$TaS_{2-x}Se_x$, and what is the dissimilarity or universality if compared with those of pristine $1T$-TaS_2 under high pressure[11] and $1T$-$Fe_xTa_{1-x}S_2$.[13,14] On the other hand, it is imperative to unveil whether substantial deviation and anomaly beyond the conventional Peierls picture occurs between the CCDW Mott insulating phase in $1T$-TaS_2[10,16–19] and the isostructural CCDW metallic phase in $1T$-$TaSe_2$.[5,20–22] As a matter of fact, previous attempts have been made to clarify the fundamental nature of the ground state in pristine $1T$-$TaSe_2$, while it still remains highly controversial.[20,22–25] It is thus of great importance to experimentally elucidate the entire evolution of electronic structure in $1T$-$TaS_{2-x}Se_x$ ($0 \leqslant x \leqslant 2.0$). In this work, we report high-resolution angle-resolved photoemission spectroscopy (ARPES) of $1T$-$TaS_{2-x}Se_x$. Our most important finding is the direct comparison of the electronic states with different characteristics for superconductivity and Mott metal-insulator transition, suggesting the importance of effective electron correlation and p-d hybridization for realizing the superconductivity and bandwidth-controlled Mott metal-insulator transition.

II. EXPERIMENT

High-quality single crystals of $1T$-$TaS_{2-x}Se_x$ ($0 \leqslant x \leqslant 2.0$) were grown by the chemical vapor transport technique with iodine as a transport agent. Details of the sample preparation were described elsewhere.[15] ARPES measurements were performed using a VG-SCIENTA SES2002 spectrometer with a high-flux He discharge lamp at Tohoku University. The He-Iα ($h\nu = 21.218$ eV) resonance line was used to excite photoelectrons. The samples were cleaved *in situ* in an ultrahigh vacuum better than 5×10^{-11} Torr. The energy and angular (k) resolutions were set at 13 meV and 0.2° (0.007 $Å^{-1}$), respectively. The Fermi level (E_F) of the samples was referenced to that of a gold film evaporated onto the sample holder. The low-energy electron diffraction (LEED) pattern was used to check the sample orientation and the CDW superstructure.

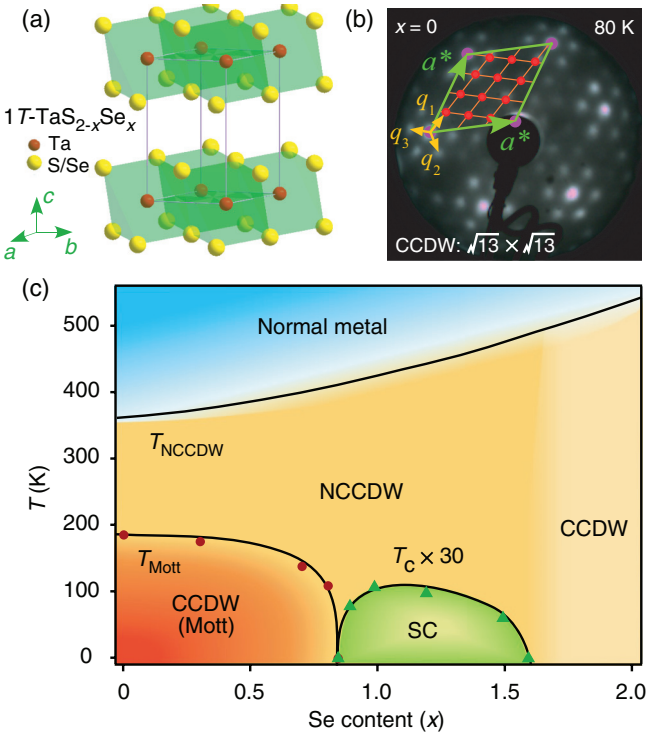

FIG. 1. (Color online) (a) Crystal structure of $1T$-$TaS_{2-x}Se_x$. (b) LEED pattern of the $\sqrt{13} \times \sqrt{13}$ superstructure with an electron energy 105 eV measured at 80 K in pristine $1T$-TaS_2 ($x = 0$), where wave vector $q = 1/\sqrt{13}a^*$. (c) Schematic electronic phase diagram of $1T$-$TaS_{2-x}Se_x$ derived from transport properties[15] as a function of temperature and x, where CCDW, NCCDW, and SC represents the commensurate CDW, nearly commensurate CDW, and superconductivity, respectively. For the optimal sample $x = 1.0$, the SC critical temperature T_c is 3.5 K.

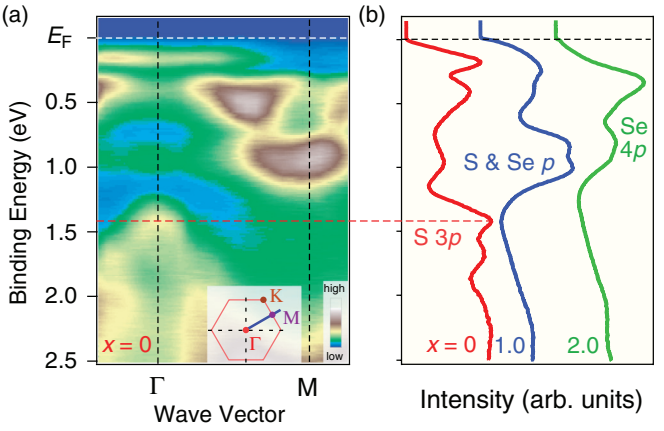

FIG. 2. (Color online) (a) Valence-band ARPES intensity of pristine $1T$-TaS_2 ($x = 0$) along the ΓM direction, plotted as a function of wave vector and binding energy at $T = 30$ K. (b) Comparison of ARPES spectra at the Fermi vector k_F point around the Γ point for $x = 0$, 1.0, and 2.0 at $T = 30$ K.

III. RESULTS AND DISCUSSION

To elucidate the overall characteristics of the valence band (VB) in $1T$-$TaS_{2-x}Se_x$, first we performed high-resolution ARPES measurements at $T = 30$ K. Figure 2(a) shows the plot of ARPES intensity along the ΓM cut for pristine $1T$-TaS_2 ($x = 0$). It is to be stressed that here we pay attention to the band dispersion for chalcogen p orbitals around the Γ point, while previous ARPES investigation[7,10,19,26–29] mainly focused on the Mott-gap opening at ~0.2 eV driven by the Ta $5d$ orbital. As shown in Fig. 2(a), one holelike band at ~1.4 eV is clearly visible around the Γ point, which is a feature of the S $3p$ orbital, in agreement with the band calculations.[9,30,31] Figure 2(b) presents the corresponding energy distribution curves (EDCs) at the Fermi vector (k_F) point around the Γ point. We observed a peak of S $3p$ at ~1.4 eV (see EDC marked by a red dashed line). More importantly, besides the band dispersion of the Ta $5d$ orbital near E_F, the Se $4p$ orbital is gradually close to E_F for pristine $1T$-$TaSe_2$ ($x = 2.0$), which is a hallmark of p-d hybridization. We will discuss implications of this observation later in detail.

To gain further insight into the distinct evolution of electronic states near E_F, Figs. 3(a) and 3(b) display a systematic comparison of EDCs and corresponding second-derivative ARPES intensity plots around the Γ point at $T = 30$ K involving the CCDW Mott insulating phase ($x = 0$, 0.3, and 0.8), the NCCDW phase ($x = 0.9$, 1.0, 1.3, and 1.6), and the CCDW metallic phase ($x = 1.8$ and 2.0). Apparently, at $x = 0.9$, there is an electronlike feature whose bottom is ~0.2 eV below E_F. This single electron pocket eventually evolves into two folded bands at high x values of $x \sim 1.3$–1.6, which is likely due to the stronger superlattice potential of NCCDW for higher x. These observations are essentially similar to previous Fe-substituted $1T$-$Fe_xTa_{1-x}S_2$.[14] Hence the superconductivity of $1T$-$TaS_{2-x}Se_x$ is likely characterized by the electron pocket with band folding.

Another intriguing finding is the distinct difference in electronic states between the CCDW Mott insulating state and the CCDW metallic state [see Figs. 3(a) and 3(b)]. As a whole, the observed electronic states look quite analogous between $x = 0$–0.8 and 1.8–2.0, which is commonly presented as two "M-shaped" band dispersions around the Γ point. But a careful look at Figs. 3(a) and 3(b) further reveals that there are two considerable disparities: in (i) the larger energy gap opening for $x = 1.8$–2.0 in comparison with $x = 0$–0.8 and (ii) the finite ARPES intensity in the vicinity of E_F for $x = 1.8$–2.0, while ARPES intensity at E_F is absent for $x = 0$–0.8. The pronounced intensity near E_F for $x = 1.8$–2.0 would be accountable to the metallic behavior, in accordance with the transport properties.[15] As also visible in Figs. 3(c) and 3(d), the spectra at E_F for $x = 1.8$–2.0 and 0–0.8 reveals the intrinsic difference between metallic and insulating phases. By contrast, the line shape is not gapped and exhibits a metallic edge at E_F for $x = 1.8$–2.0, while such a feature is absent for $x = 0$–0.8.

Now we discuss the implications between the CCDW insulating phase of $1T$-TaS_2 and the CCDW metallic phase of $1T$-$TaSe_2$. From the viewpoint of superstructure, the CCDW phase of $1T$-TaS_2 is identical to that of $1T$-$TaSe_2$, since both show $\sqrt{13} \times \sqrt{13}$ symmetry.[5,6,21,32,33] Nevertheless, the matter of concern is how to precisely distinguish the origin of the insulating phase of $1T$-TaS_2 and the metallic phase of $1T$-$TaSe_2$. As highlighted from the present ARPES result, the Mott gap opening of $1T$-TaS_2 (defined as E_{Mott}) is well comprehended as the lower Hubbard band (LHB);[10,28,29] it is

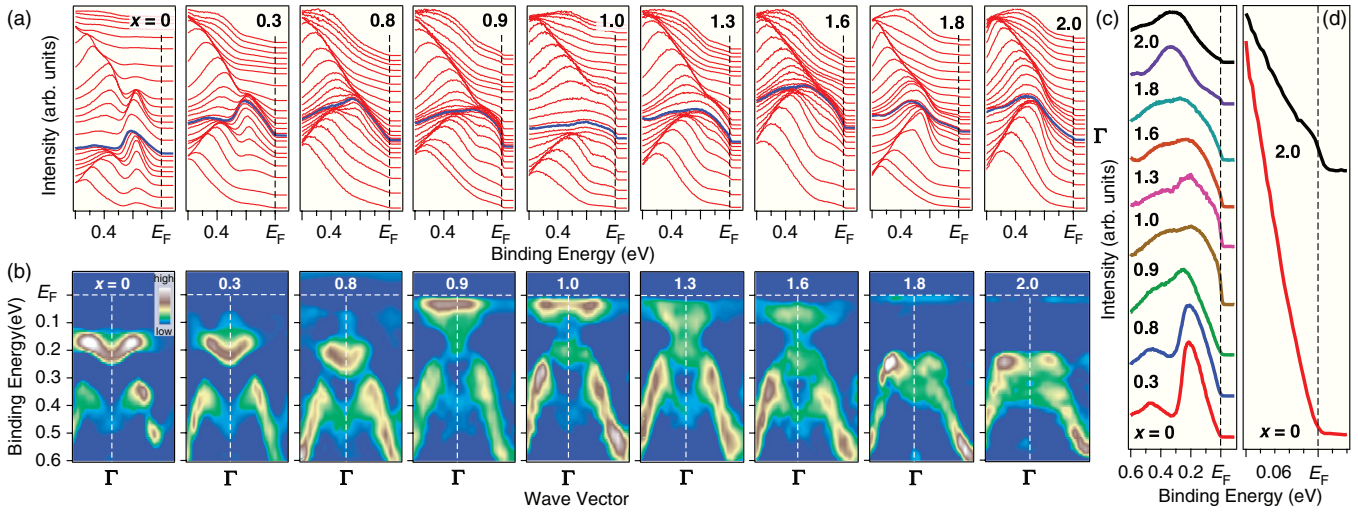

FIG. 3. (Color online) (a) x dependence of EDCs around the Γ point in $1T$-$TaS_{2-x}Se_x$ at $T = 30$ K. (b) Corresponding second-derivative ARPES intensity plot as a function of wave vector and binding energy. (c) Comparison of ARPES spectra at the Γ point. (d) Expanded view near E_F for $x = 0$ and 2.0 shown in (c).

thus natural to conclude that the large E_{Mott} value of $1T$-$TaSe_2$ is also reflected by the LHB due to the strong electron correlation, since the Mott gap opening of $1T$-TaS_2 was found on the verge of the SC region [see Fig. 1(c)] as well as $1T$-$TaSe_2$. On the other hand, the theoretical calculations[30,34] have indicated the strong overlap of Ta $5d$ and Se $4p$ derived bands in $1T$-$TaSe_2$, demonstrating the characteristic of p-d orbital hybridization based on our ARPES results (see also Fig. 2). It is thus reasonable to conclude that the Ta $5d$ orbital contributes to the LHB with large E_{Mott} value, while the Se $4p$ orbital is responsible for the unconventional metallic phase, coinciding with the near-E_F intensity in ARPES experiment, revealing the orbital dependent physics, i.e., the orbital-selective Mott transition (OSMT). In this regard, there is a possibility for the localization of part of the Ta $5d$ conduction electrons, while the rest, the Se $4p$ part, remains itinerant. In fact, we also checked the electronic state of $1T$-$TaSe_2$ at room temperature, and found that the pronounced intensity still persists near E_F, confirming the metallic behavior in the CCDW phase. This is contrary to the previous argument,[22,23] where the metal-insulator transition in the CCDW phase was believed to occur at the surface state of the samples between room temperature and low temperature in $1T$-$TaSe_2$. Unambiguously, our finding supports the unique metallic ground state of $1T$-$TaSe_2$ in the whole CCDW phase, in line with the transport properties.[15]

The next issue to be clarified is the connection between the superconductivity and the Mott metal-insulator transition. As shown in Fig. 4(a), the E_{Mott} value apparently has an anticorrelation behavior with the density of states (DOS) at E_F; when the E_{Mott} value becomes zero, the DOS increases and the DOS looks to follow the SC dome shape. This strongly suggests that the SC and the Mott state compete with each other. Meanwhile, it was found that the E_{Mott} value of $x = 1.8$–2.0 is much larger than that for $x = 0$–0.8, suggesting the stronger electron correlation effect for the former. On the other hand, the variation of DOS strongly indicates the substantial disparity of the superconductivity and the Mott metal-insulator transition. We pay attention to the survival of DOS for Se rich samples, further supporting the occurrence of unusual metallic behavior. Figure 4(b) shows the band

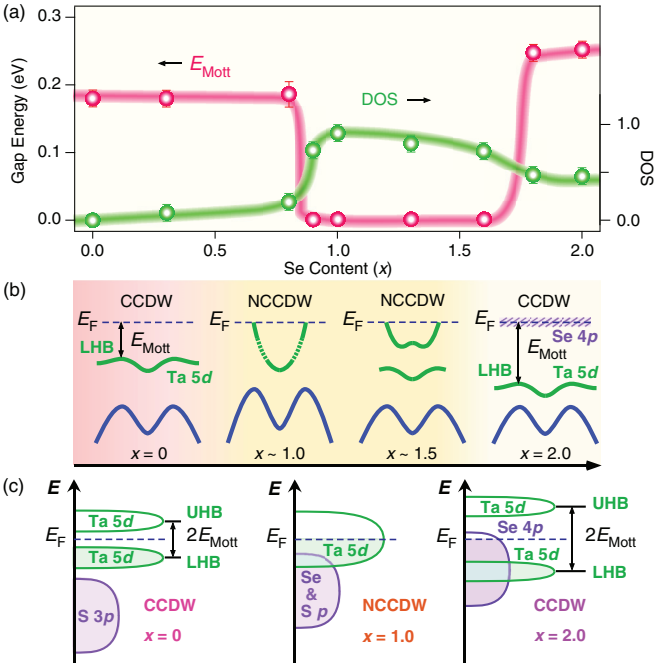

FIG. 4. (Color online) (a) Gap energy (the Mott gap E_{Mott}) and density of states (DOS) at E_F of an electron pocket with folding bands plotted as a function of x. The E_{Mott} value was estimated by the peak position of the EDC at the minimum-gap momentum k locus of the weakly dispersing lower Hubbard band (LHB). The DOS at E_F is estimated by the intensity at E_F of EDCs integrated along the ΓM direction, normalized to the 0.4 eV peak. (b) Schematic band diagram derived from the present ARPES experiment as a function of x. Dashed curve represents the absence of the band. Purple shadow region expresses the crossing of Se $4p$ orbital at E_F. (c) Schematic orbital characters derived from the present ARPES experiment as a function of x, where UHB and E_{Mott} represents the upper Hubbard band and Mott-Hubbard gap, respectively.

picture for different electronic phases determined from the present ARPES result. The electron pocket appears only in the NCCDW phase as well as the superconductivity. The electron pocket is gapped in the Mott phase (i.e., Mott metal-insulator transition) due to the enhanced electron correlation, implying the competing nature of the superconductivity with Mott phase. Noticeably, the splitted folded bands for $x = 0.9$–1.6 confirm the gradual decrease of bandwidth W. This certainly enhances the ratio of effective electron correlation (U/W) in the NCCDW state, where U is the on-site Coulomb interaction, which is crucial for elucidating the larger Mott-gap opening of CCDW. Figure 4(c) summarizes the evolution of electronic states in the CCDW Mott insulating phase, the superconductivity, and the CCDW metal phase. For the CCDW Mott insulator, the E_{Mott} opens between the LHB and the upper Hubbard band (UHB), while the S $3p$ orbital is far away from the Ta $5d$ orbital leading to very small p-d hybridization. Due to the electron-electron interaction, the Ta $5d$ orbital is split into an unoccupied UHB and a corresponding LHB. The LHB is manifest as a dispersionless peak near E_{F} in the CCDW insulating phase. For the NCCDW phase, the Se $4p$ orbital shifts towards E_{F} and overlaps with the Ta $5d$ orbital, accompanied by the formation of an electron pocket which is associated with the superconductivity. The electron pocket is characteristic of the NCCDW phase and the SC phase, and likely created by the backfolding of bands due to the superlattice potential of NCCDW, indicative of the coexistence of the NCCDW and the superconductivity in real space. In the CCDW metal phase, the E_{Mott} opens again between the LHB and the UHB, while the Se $4p$ band crosses E_{F} and the p-d hybridization further enhances. As mentioned above, the scenario of OSMT is proposed to account for the localized Ta $5d$ and itinerant Se $4p$ electrons. In comparison with $1T$-TaS_2, the isovalent Se substitute does not change the total carrier concentration, but rather increases the ratio of U/W which is induced by lattice distortion due to the larger ion radius of Se. Consequently, it is possible that an OSMT takes place in $1T$-$TaSe_2$, i.e., the Ta $5d$ electrons undergo a Mott transition and become localized, while the Se $4p$ electrons remain itinerant. The OSMT mechanism is also reminiscent of the single-layer ruthenates $Ca_{2-x}Sr_xRuO_4$[35,36] and heavy fermion materials such as UPd_2Al_3.[37] Our result thus sheds a light on this controversial issue in ruthenates and a heavy fermion system by providing a new material platform elucidating the OSMT physics.

Finally, we compare and discuss the prominent dissimilarity and universality among the present ARPES experiment of $1T$-$TaS_{2-x}Se_x$ ($0 \leqslant x \leqslant 2.0$), the previous high-pressure experiment of pristine $1T$-TaS_2,[11] and the previous ARPES experiment of $1T$-$Fe_xTa_{1-x}S_2$ ($0 \leqslant x \leqslant 0.05$).[14] For the high-pressure case, it was proposed that the superconductivity forms within the metallic interdomain spaces of the NCCDW phase,[11] while our ARPES experiment of $1T$-$TaS_{2-x}Se_x$ suggests the real-space coexistence of the superconductivity and the NCCDW, as well as that of $1T$-$Fe_xTa_{1-x}S_2$.[14] Actually, the emergence of superconductivity is not dependent on the substitution S or Ta site. The superconductivity of both $1T$-$TaS_{2-x}Se_x$ and $1T$-$Fe_xTa_{1-x}S_2$ is likely characterized by the electron pocket with band folding, demonstrating the universal nature of $1T$-TaS_2 systems. Nevertheless, for lightly Fe-substituted $1T$-$Fe_xTa_{1-x}S_2$, the strong disorder dominates the electronic states spanned by the Anderson localization;[13] the ratio of U/W cannot freely tune the Mott insulator and the superconductivity, peculiarly noting the fact that no evidence indicates the dominant contribution of the Fe $3d$ orbital near E_{F}, but the robust Ta $5d$ orbital plays a pivotal role to the occurrence of superconductivity, particularly without consideration of the p-d hybridization.[14] Conversely, for the present solid-solution system $1T$-$TaS_{2-x}Se_x$, the ratio of U/W controls the electronic states at low temperatures, while the disorder may have a less important contribution. Also, the U/W can effectively modulate the superconductivity and Mott metal-insulator transition. Very contrastingly, taking into account the strong p-d hybridization, it is suggested that the Ta $5d$ orbital attends to materialize the superconductivity, while the Se $4p$ orbital is responsible for the unconventional metallic behavior for Se rich samples.

IV. CONCLUSION

In conclusion, we have performed high-resolution ARPES experiments on $1T$-$TaS_{2-x}Se_x$ to elucidate the energy-band structure relevant to the emergence of superconductivity and the bandwidth-controlled Mott metal-insulator transition. We found that the superconductivity is characterized by the electron pocket deriving from the Ta $5d$ orbital, which is destroyed by a Mott-gap opening in the insulating ground state for S rich samples. Especially, the enhanced electron-electron interaction-induced Mott gap driven by the Ta $5d$ orbital also exists in the metallic ground state for Se-rich samples, accompanied by the survival of finite near-E_{F} intensity likely arising from the Se $4p$ orbital, revealing the nature of OSMT. Present results suggest the importance of effective electron correlation and p-d hybridization for realizing the superconductivity and Mott physics.

ACKNOWLEDGMENTS

We thank K. Sugawara for his assistance in the experiment of LEED pattern. This work was supported by grants from the Japan Society for the Promotion of Science, Japan Science and Technology Agency-Core Research for Evolutional Science and Technology, Ministry of Education, Culture, Sports, Science, and Technology of Japan, WPI Research Center, Advanced Institute for Materials Research of Japan, National Key Basic Research of China under Contract No. 2011CBA00111, and the Joint Funds of the National Natural Science Foundation of China and the Chinese Academy of Sciences Large-scale Scientific Facility (Grant No. U1232139).

*Corresponding author: r.ang@arpes.phys.tohoku.ac.jp

[1] D. S. Chow, F. Zamborszky, B. Alavi, D. J. Tantillo, A. Baur, C. A. Merlic, and S. E. Brown, Phys. Rev. Lett. **85**, 1698 (2000).

[2] K. Hiraki and K. Kanoda, Phys. Rev. Lett. **80**, 4737 (1998).

[3] E. Dagotto, Rev. Mod. Phys. **66**, 763 (1994).

[4]A. Damascelli, Z. Hussain, and Z. X. Shen, Rev. Mod. Phys. **75**, 473 (2003).
[5]J. A. Wilson, F. J. Di Salvo, and S. Mahajan, Adv. Phys. **24**, 117 (1975).
[6]P. Fazekas and E. Tosatti, Philos. Mag. B **39**, 229 (1979); Physica B & C **99**, 183 (1980).
[7]R. Manzke, T. Buslaps, B. Pfalzgraf, M. Skibowski, and O. Anderson, Europhys. Lett. **8**, 195 (1989).
[8]R. E. Thomson, B. Burk, A. Zettl, and J. Clarke, Phys. Rev. B **49**, 16899 (1994).
[9]Th. Pillo, J. Hayoz, H. Berger, R. Fasel, L. Schlapbach, and P. Aebi, Phys. Rev. B **62**, 4277 (2000).
[10]L. Perfetti, P. A. Loukakos, M. Lisowski, U. Bovensiepen, H. Berger, S. Biermann, P. S. Cornaglia, A. Georges, and M. Wolf, Phys. Rev. Lett. **97**, 067402 (2006).
[11]B. Sipos, A. F. Kusmartseva, A. Akrap, H. Berger, L. Forro, and E. Tutis, Nat. Mater. **7**, 960 (2008).
[12]P. Xu, J. O. Piatek, P.-H. Lin, B. Sipos, H. Berger, L. Forro, H. M. Ronnow, and M. Grioni, Phys. Rev. B **81**, 172503 (2010).
[13]L. J. Li, W. J. Lu, X. D. Zhu, L. S. Ling, Z. Qu, and Y. P. Sun, Europhys. Lett. **97**, 67005 (2012).
[14]R. Ang, Y. Tanaka, E. Ieki, K. Nakayama, T. Sato, L. J. Li, W. J. Lu, Y. P. Sun, and T. Takahashi, Phys. Rev. Lett. **109**, 176403 (2012).
[15]Y. Liu, R. Ang, W. J. Lu, W. H. Song, L. J. Li, and Y. P. Sun, Appl. Phys. Lett. **102**, 192602 (2013).
[16]S. Hellmann, M. Beye, C. Sohrt, T. Rohwer, F. Sorgenfrei, H. Redlin, M. Kalläne, M. Marczynski-Bühlow, F. Hennies, M. Bauer, A. Föhlisch, L. Kipp, W. Wurth, and K. Rossnagel, Phys. Rev. Lett. **105**, 187401 (2010).
[17]M. Eichberger, H. Schafer, M. Krumova, M. Beyer, J. Demsar, H. Berger, G. Moriena, G. Sciaini, and R. J. D. Miller, Nature (London) **468**, 799 (2010).
[18]K. Ishizaka, T. Kiss, T. Yamamoto, Y. Ishida, T. Saitoh, M. Matsunami, R. Eguchi, T. Ohtsuki, A. Kosuge, T. Kanai, M. Nohara, H. Takagi, S. Watanabe, and S. Shin, Phys. Rev. B **83**, 081104 (R) (2011).
[19]J. C. Petersen, S. Kaiser, N. Dean, A. Simoncig, H. Y. Liu, A. L. Cavalieri, C. Cacho, I. C. E. Turcu, E. Springate, F. Frassetto, L. Poletto, S. S. Dhesi, H. Berger, and A. Cavalleri, Phys. Rev. Lett. **107**, 177402 (2011).
[20]K. Horiba, K. Ono, J. H. Oh, T. Kihara, S. Nakazono, M. Oshima, O. Shiino, H. W. Yeom, A. Kakizaki, and Y. Aiura, Phys. Rev. B **66**, 073106 (2002).
[21]H. J. Crawack and C. Pettenkofer, Solid State Commun. **118**, 325 (2001).
[22]S. Colonna, F. Ronci, A. Cricenti, L. Perfetti, H. Berger, and M. Grioni, Phys. Rev. Lett. **94**, 036405 (2005).
[23]L. Perfetti, A. Georges, S. Florens, S. Biermann, S. Mitrovic, H. Berger, Y. Tomm, H. Hochst, and M. Grioni, Phys. Rev. Lett. **90**, 166401 (2003).
[24]O. Shiino, T. Endo, W. Yamaguchi, H. Sugawara, K. Kitazawa, and T. Hasegawa, Appl. Phys. A **66**, S175 (1998).
[25]S. Colonna, F. Ronci, A. Cricenti, L. Perfetti, H. Berger, and M. Grioni, Jpn. J. Appl. Phys. **45**, 1950 (2006).
[26]N. V. Smith, S. D. Kevan, and F. J. DiSalvo, J. Phys. C: Solid State Phys. **18**, 3175 (1985).
[27]Th. Pillo, J. Hayoz, H. Berger, M. Grioni, L. Schlapbach, and P. Aebi, Phys. Rev. Lett. **83**, 3494 (1999).
[28]F. Zwick, H. Berger, I. Vobornik, G. Margaritondo, L. Forro, C. Beeli, M. Onellion, G. Panaccione, A. Taleb-Ibrahimi, and M. Grioni, Phys. Rev. Lett. **81**, 1058 (1998).
[29]L. Perfetti, T. A. Gloor, F. Mila, H. Berger, and M. Grioni, Phys. Rev. B **71**, 153101 (2005).
[30]M. Bovet, S. van Smaalen, H. Berger, R. Gaal, L. Forro, L. Schlapbach, and P. Aebi, Phys. Rev. B **67**, 125105 (2003); M. Bovet, D. Popovic, F. Clerc, C. Koitzsch, U. Probst, E. Bucher, H. Berger, D. Naumovic, and P. Aebi, *ibid*. **69**, 125117 (2004).
[31]F. Clerc, M. Bovet, H. Berger, L. Despont, C. Koitzsch, O. Gallus, L. Patthey, M. Shi, J. Krempasky, M. G. Garnier, and P. Aebi, J. Phys.: Condens. Matter **16**, 3271 (2004).
[32]C. B. Scruby, P. M. Williams, and G. S. Parry, Philos. Mag. **31**, 255 (1975).
[33]A. M. Woolley and G. Wexler, J. Phys. C: Solid State Phys. **10**, 2601 (1977).
[34]A. H. Reshak and S. Auluck, Physica B **358**, 158 (2005).
[35]V. I. Anisimov, I. A. Nekrasov, D. E. Kondakov, T. M. Rice, and M. Sigrist, Eur. Phys. J. B **25**, 191 (2002).
[36]A. Koga, N. Kawakami, T. M. Rice, and M. Sigrist, Phys. Rev. Lett. **92**, 216402 (2004).
[37]N. K. Sato, N. Aso, K. Miyake, R. Shiina, P. Thalmeier, G. Varelogiannis, C. Geibel, F. Steglich, P. Fulde, and T. Komatsubaras, Nature (London) **410**, 340 (2001).